JACS ARTICLES

Published on Web 05/11/2010

Oligopyrenotides: Abiotic, Polyanionic Oligomers with Nucleic Acid-like Structural Properties

Robert Häner,* Florian Garo, Daniel Wenger, and Vladimir L. Malinovskii

Department of Chemistry and Biochemistry, University of Bern, Freiestrasse 3, CH-3012 Bern, Switzerland

Received March 10, 2010; E-mail: robert.haener@ioc.unibe.ch

Abstract: Oligopyrenotides, abiotic oligomers that exhibit significant structural analogies to the nucleic acids, are described. They are composed of achiral, phosphodiester-linked pyrene building blocks and a single chiral 1,2-diaminocyclohexane unit. These oligomers form stable hybrids in aqueous solution. Hybridization is based on stacking interactions of the pyrene building blocks. They show thermal denaturation/renaturation behavior that closely resembles DNA and RNA hybridization. In addition, oligopyrenotides display salt-concentration-dependent structural polymorphism. Thus, they possess a number of structural attributes that are typical of nucleic acids and therefore may serve as model systems for the design of artificial self-replicating systems.

Introduction

The past two decades have seen considerable advancement in the de novo creation of helical structures.[1−8] A fair number of descriptions of synthetic helical systems inspired by peptides[9−12] and DNA[13−20] exist in the literature. Nucleic acids occur in single and multistranded helical architectures[21−24] and thereby serve as role models for the design of artificial helical systems.[10,20,25−31] In these artificial assemblies, the interaction between strands is largely controlled by formation of hydrogen bonds or metal chelates between heteroaromatic bases. Non-hydrogen-bonded base pairs have been investigated in the context of punctually or partially modified DNAs,[32−49] yet no reports of nucleotide-independent systems exist in the literature.

(1) Gellman, S. H. *Acc. Chem. Res.* **1998**, *31*, 173–180.
(2) Piguet, C.; Bernardinelli, G.; Hopfgartner, G. *Chem. Rev.* **1997**, *97*, 2005–2062.
(3) Lokey, R. S.; Iverson, B. L. *Nature* **1995**, *375*, 303–305.
(4) Berl, V.; Huc, I.; Khoury, R. G.; Krische, M. J.; Lehn, J. M. *Nature* **2000**, *407*, 720–723.
(5) Hill, D. J.; Mio, M. J.; Prince, R. B.; Hughes, T. S.; Moore, J. S. *Chem. Rev.* **2001**, *101*, 3893–4011.
(6) Huc, I. *Eur. J. Org. Chem.* **2004**, *1*, 7–29.
(7) Palmans, A. R. A.; Meijer, E. W. *Angew. Chem., Int. Ed.* **2007**, *46*, 8948–8968.
(8) Haldar, D.; Schmuck, C. *Chem. Soc. Rev.* **2009**, *38*, 363–371.
(9) Nelson, J. C.; Saven, J. G.; Moore, J. S.; Wolynes, P. G. *Science* **1997**, *277*, 1793–1796.
(10) Yashima, E.; Maeda, K.; Furusho, Y. *Acc. Chem. Res.* **2008**, *41*, 1166–1180.
(11) Cheng, R. P.; Gellman, S. H.; DeGrado, W. F. *Chem. Rev.* **2001**, *101*, 3219–3232.
(12) Seebach, D.; Cardiner, J. *Acc. Chem. Res.* **2008**, *41*, 1366–1375.
(13) Eschenmoser, A. *Science* **1999**, *284*, 2118–2124.
(14) Schneider, K. C.; Benner, S. A. *J. Am. Chem. Soc.* **1990**, *112*, 453–455.
(15) Nielsen, P. E.; Haaima, G. *Chem. Soc. Rev.* **1997**, *26*, 73–78.
(16) Herdewijn, P. *Biochim. Biophys. Acta* **1999**, *1489*, 167–179.
(17) Kool, E. T. *Acc. Chem. Res.* **2002**, *35*, 936–943.
(18) Leumann, C. J. *Bioorg. Med. Chem.* **2002**, *10*, 841–854.
(19) Zhang, L. L.; Peritz, A.; Meggers, E. *J. Am. Chem. Soc.* **2005**, *127*, 4174–4175.
(20) Tanaka, K.; Clever, G. H.; Takezawa, Y.; Yamada, Y.; Kaul, C.; Shionoya, M.; Carell, T. *Nat. Nanotechnol.* **2006**, *1*, 190–194.
(21) Murchie, A. I. H.; Lilley, D. M. *Methods Enzymol.* **1992**, *211*, 158–180.
(22) Saenger, W. *Principles of Nucleic Acid Structure*; Springer-Verlag: New York, 1984.
(23) Bloomfield, V. A.; Crothers, D. M.; Tinoco, I., Jr. *Nucleic Acids: Structures, Properties, and Functions*; University Science Books: Sausalito, CA, 2000.
(24) Gilbert, D. E.; Feigon, J. *Curr. Opin. Struct. Biol.* **1999**, *9*, 305–314.
(25) Albrecht, M. *Angew. Chem., Int. Ed.* **2005**, *44*, 6448–6451.
(26) Benner, S. A. *Acc. Chem. Res.* **2004**, *37*, 784–797.
(27) Benner, S. A.; Sismour, A. M. *Nat. Rev. Genet.* **2005**, *6*, 533–543.
(28) Ogawa, A. K.; Wu, Y. Q.; McMinn, D. L.; Liu, J. Q.; Schultz, P. G.; Romesberg, F. E. *J. Am. Chem. Soc.* **2000**, *122*, 3274–3287.
(29) Schlegel, M. K.; Zhang, L. L.; Pagano, N.; Meggers, E. *Org. Biomol. Chem.* **2009**, *7*, 476–482.
(30) Clever, G. H.; Kaul, C.; Carell, T. *Angew. Chem., Int. Ed.* **2007**, *46*, 6226–6236.
(31) Wengel, J. *Org. Biomol. Chem.* **2004**, *2*, 277–280.
(32) Matray, T. J.; Kool, E. T. *J. Am. Chem. Soc.* **1998**, *120*, 6191–6192.
(33) Mathis, G.; Hunziker, J. *Angew. Chem., Int. Ed.* **2002**, *41*, 3203–3205.
(34) Langenegger, S. M.; Häner, R. *Helv. Chim. Acta* **2002**, *85*, 3414–3421.
(35) Christensen, U. B.; Pedersen, E. B. *Nucleic Acids Res.* **2002**, *30*, 4918–4925.
(36) Lewis, F. D.; Zhang, L. G.; Liu, X. Y.; Zuo, X. B.; Tiede, D. M.; Long, H.; Schatz, G. C. *J. Am. Chem. Soc.* **2005**, *127*, 14445–14453.
(37) Kashida, H.; Asanuma, H.; Komiyama, M. *Angew. Chem., Int. Ed.* **2004**, *43*, 6522–6525.
(38) Malinovskii, V. L.; Samain, F.; Häner, R. *Angew. Chem., Int. Ed.* **2007**, *46*, 4464–4467.
(39) Bittermann, H.; Siegemund, D.; Malinovskii, V. L.; Häner, R. *J. Am. Chem. Soc.* **2008**, *130*, 15285–15287.
(40) Bouquin, N.; Malinovskii, V. L.; Häner, R. *Chem. Commun.* **2008**, 1974–1976.
(41) Baumstark, D.; Wagenknecht, H. A. *Chem.—Eur. J.* **2008**, *14*, 6640–6645.
(42) Bouquin, N.; Malinovskii, V. L.; Guégano, X.; Liu, S.-X.; Decurtins, S.; Häner, R. *Chem.—Eur. J.* **2008**, *14*, 5732–5736.
(43) Zahn, A.; Leumann, C. J. *Chem.—Eur. J.* **2008**, *14*, 1087–1094.
(44) Uno, S.; Dohno, C.; Bittermann, H.; Malinovskii, V. L.; Häner, R.; Nakatani, K. *Angew. Chem., Int. Ed.* **2009**, *48*, 7362–7365.
(45) Hainke, S.; Seitz, O. *Angew. Chem., Int. Ed.* **2009**, *48*, 8250–8253.
(46) Häner, R.; Biner, S. M.; Langenegger, S. M.; Meng, T.; Malinovskii, V. L. *Angew. Chem., Int. Ed.* **2010**, *49*, 1227–1230.
(47) Malinovskii, V. L.; Wenger, D.; Häner, R. *Chem. Soc. Rev.* **2010**, *39*, 410–422.

 10.1021/ja102042p

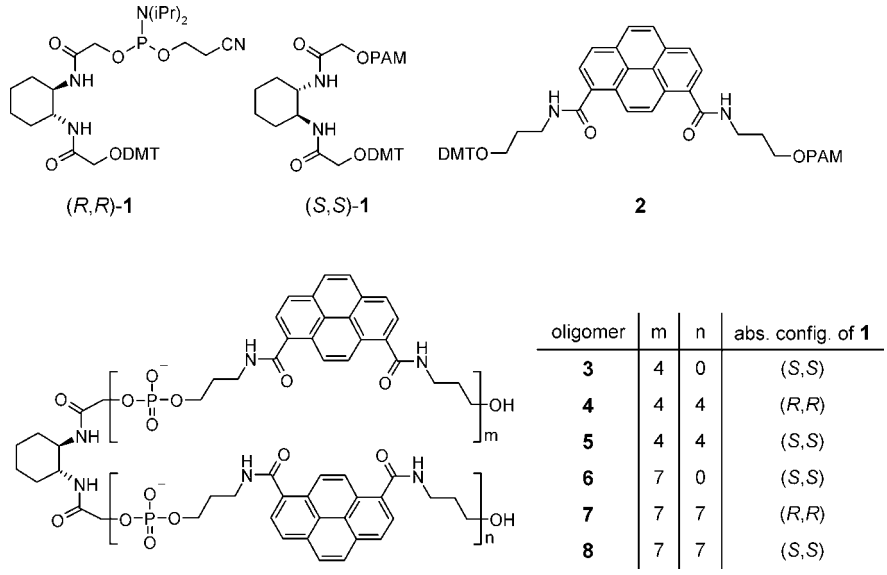

oligomer	m	n	abs. config. of **1**
3	4	0	(*S*,*S*)
4	4	4	(*R*,*R*)
5	4	4	(*S*,*S*)
6	7	0	(*S*,*S*)
7	7	7	(*R*,*R*)
8	7	7	(*S*,*S*)

Figure 1. Oligomers **3**−**8** composed of achiral pyrene building blocks and a chiral 1,2-diaminocyclohexane unit as well as the respective monomeric building blocks (PAM = phosphoramidite, as shown in (*R*,*R*)-**1**; DMT stands for 4,4′-dimethoxytrityl).

On the other hand, organized supramolecular assemblies that are primarily based on aromatic stacking interactions play an important role in the development of novel types of materials.[50,51] These systems are based either on the interactions of monomers to form discotic stacks[52−54] or on oligomers with an uncharged backbone.[55] The importance of the polyanionic backbone for the proper functioning of DNA as a genetic material has been emphasized previously.[56] Fully artificial oligomers composed of non-hydrogen-bonding aromatic stacking moieties assembled on a polyanionic backbone, however, have not been reported. We report here that a simple, aromatic oligophosphate exhibits structural features typically observed in nucleic acids. Polyanionic pyrene oligomers form water-soluble helical hybrids displaying salt-dependent structural polymorphism. In contrast to nucleic acids, however, the interaction of individual strands does not involve complementary hydrogen bonding but instead relies on interstrand stacking of pyrenes.

Results and Discussion

Design of Oligomers. As in nucleic acids, individual units are linked by phosphodiester groups. The nucleobases are replaced by pyrene units, and flexible aliphatic linkers are used in place of the natural ribose or deoxyribose (Figure 1). The aromatic nature of the pyrenes favors stacking interactions between the building blocks, while the propyl linkers possess enough flexibility to allow unhindered self-assembly. Solubility in water is ensured by hydrophilic phosphodiester groups. Since the pyrene components are achiral, a single chiral building block, either a (1*S*,2*S*)- or (1*R*,2*R*)-1,2-diaminocyclohexane unit,[57] is introduced into the oligomer. This unit serves as the source of chiral information according to which the oligopyrene strands adopt a preferred helical sense (see below). The corresponding phosphoramidites [**1**; see the Supporting Information (SI)] and the pyrene building block (**2**)[58−60] are shown in Figure 1. Oligomerization was performed on a DNA synthesizer by phosphoramidite chemistry[61] using a pyrene-functionalized polystyrene support (see the SI). Oligomers **3**− **8** were obtained after reversed-phase HPLC purification.

Spectroscopic Investigation. Initial analysis of the oligomers by absorption and circular dichroism (CD) spectroscopy showed no signs of defined structures at low sodium chloride concentrations (<0.75 M). Above this concentration, however, structural organization became evident (see the SI). Up to ∼2 M NaCl, the magnitude of the Cotton effects grew with increasing salt concentration. Further augmentation of the salt concentration (up to 4.0 M NaCl) resulted in a major structural change, as evidenced by CD spectroscopy. This behavior is illustrated in Figure 2a, which shows the CD spectrum of oligomer **5**. The spectra taken at 1.5 and 3.0 M NaCl are approximately mirror-inverted, indicating a switch in overall helicity.[62,63] Vibronic structures in the UV−vis spectra (Figure 2a) indicate well-defined pyrene conformations. The relative intensities of the vibronic bands were affected by ionic strength. The fluorescence spectra (Figure 2b) show the expected broad pyrene excimer band. The maximum of this band was blue-shifted with increasing oligomer concentration (e.g., from 512 to 502 nm for 0.25 and 6.0 μM oligomer, respectively, at 1.5 M NaCl). A

(48) Filichev, V. V.; Pedersen, E. B. DNA-Conjugated Organic Chromophores in DNA Stacking Interactions. In *Wiley Encyclopedia of Chemical Biology*; Begley, T. P., Ed.; Wiley: Hoboken, NJ, 2009; Vol. 1, pp 493−524.
(49) Endo, M.; Sugiyama, H. *ChemBioChem* **2009**, *10*, 2420–2443.
(50) Grimsdale, A. C.; Müllen, K. *Macromol. Rapid Commun.* **2007**, *28*, 1676–1702.
(51) Anthony, J. E. *Angew. Chem., Int. Ed.* **2008**, *47*, 452–483.
(52) Chen, Z. J.; Lohr, A.; Saha-Möller, C. R.; Würthner, F. *Chem. Soc. Rev.* **2009**, *38*, 564–584.
(53) Drain, C. M.; Varotto, A.; Radivojevic, I. *Chem. Rev.* **2009**, *109*, 1630–1658.
(54) Hoeben, F. J. M.; Jonkheijm, P.; Meijer, E. W.; Schenning, A. P. H. J. *Chem. Rev.* **2005**, *105*, 1491–1546.
(55) Grimsdale, A. C.; Chan, K. L.; Martin, R. E.; Jokisz, P. G.; Holmes, A. B. *Chem. Rev.* **2009**, *109*, 897–1091.
(56) Benner, S. A.; Hutter, D. *Bioorg. Chem.* **2002**, *30*, 62–80.
(57) Bennani, Y. L.; Hanessian, S. *Chem. Rev.* **1997**, *97*, 3161–3195.
(58) Langenegger, S. M.; Häner, R. *Chem. Commun.* **2004**, 2792–2793.
(59) Langenegger, S. M.; Häner, R. *ChemBioChem* **2005**, *6*, 848–851.
(60) Samain, F.; Malinovskii, V. L.; Langenegger, S. M.; Häner, R. *Bioorg. Med. Chem.* **2008**, *16*, 27–33.
(61) Caruthers, M. H. *Science* **1985**, *230*, 281–285.
(62) Hembury, G. A.; Borovkov, V. V.; Inoue, Y. *Chem. Rev.* **2008**, *108*, 1–73.
(63) *Circular Dichroism: Principles and Applications*, 2nd ed.; Berova, N., Nakanishi, K., Woody, R. W., Eds.; Wiley-VCH: New York, 2000.

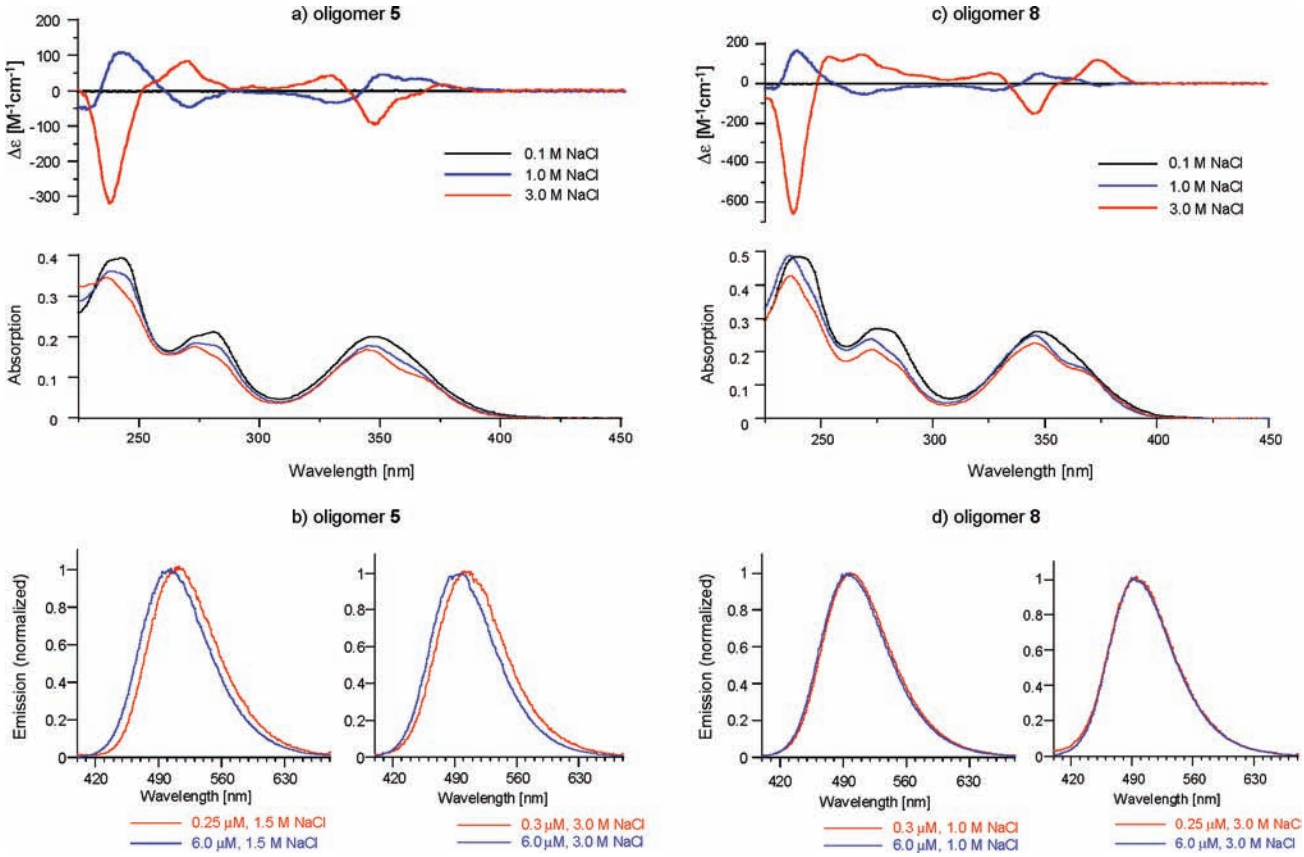

Figure 2. Spectroscopic data for (a, b) **5** and (c, d) **8** [10 mM phosphate buffer (pH 7.0), 20 °C]: (a, c) (top) CD and (bottom) UV−vis absorbance spectra at various salt concentrations (oligomer concentration: 5.0 μM for CD and 2.0 μM for UV−vis); (b, d) fluorescence spectra at various oligomer and salt concentrations.

blue shift reflects an increase in the twisting angle of the stacked pyrenes.[38,64,65] In combination with the observed CD and UV effects, this strongly supports the conclusion that oligopyrene **5** adopts a helical structure. In comparison, oligomer **3**, which has only one oligopyrene chain linked to the diaminocyclohexane, showed no vibronic bands in the UV absorbance spectra nor Cotton effects in the CD spectra (see the SI).

Oligomer **8**, which differs from **5** in the length of the pyrene chains, also revealed a high degree of structural organization (Figure 2c). The CD spectra again disclosed a strong structural dependence on ionic strength. As in the case of **5**, the curves at lower and higher ionic strength differed significantly, being almost mirror images. UV−vis absorbance supports pyrene stacking by salt-dependent changes in the vibronic band intensities, indicating reduced flexibility in the pyrene stack with increasing salt concentration (Figure 2d). At all concentrations tested, excimer emission showed a maximum at ~495 nm. This corresponds closely to the emission observed for the helical form of oligomer **5** and suggests that **8** adopts a well-ordered, helical conformation at all oligomer concentrations tested. In addition, isosbestic points observed in temperature-dependent CD spectroscopy provide evidence for a *two-state* model (Figure 3). Taken together, these data support a model in which pyrene oligomers self-associate to form helical structures with interstrand stacked pyrenes.

Consistent and reproducible spectra of oligopyrenes were ensured by including a preannealing step, similar to what is done with nucleic acids or oligonucleotides. This is illustrated by the CD and absorption curves of the same sample of oligomer **8** before and after heating (Figure 4). It is important to note that the increase in the CD signal intensities was accompanied by a decrease in the corresponding UV−vis absorption bands. This reflects tighter stacking interactions between the chromophores as the structural organization process proceeds.

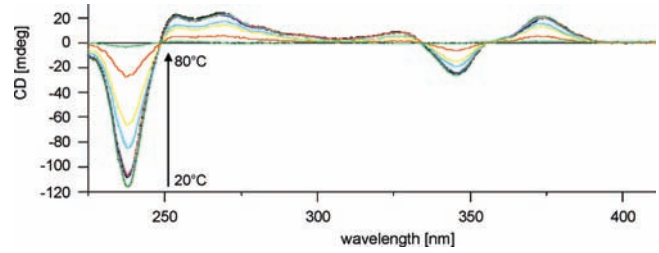

Figure 3. Temperature-dependent CD spectra of oligomer **8** [5 μM oligomer concentration, 10 mM phosphate buffer (pH 7), 3.0 M NaCl]. The arrow indicates increasing temperature (10 °C intervals).

Oligomer **6** differs from **8** in that it bears only one pyrene chain instead of two. Duplex formation of this oligomer was also supported by UV−vis, CD, and fluorescence spectroscopy (see the SI). Salt-concentration-dependent changes in the vibronic band intensities indicated pyrene stacking for **6** also. The intensity of the CD signals gradually increased with rising salt concentration, but in contrast to the behavior of oligomers **8** and **5**, the overall forms of the curves were not significantly affected by the ionic strength. The concentration-dependent excimer blue shift resulting from pyrenyl twisting was present at 1.5 M NaCl concentration but not at 3.0 M NaCl.

(64) Winnik, F. M. *Chem. Rev.* **1993**, *93*, 587–614.
(65) Häner, R.; Samain, F.; Malinovskii, V. L. *Chem.—Eur. J.* **2009**, *15*, 5701–5708.

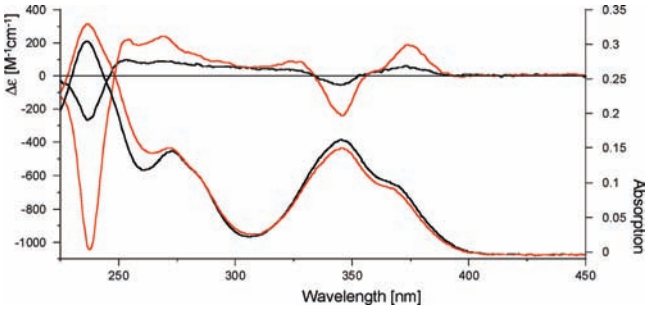

Figure 4. (top) CD and (bottom) UV−vis spectra of oligomer **8** [3.0 M NaCl, 10 mM phosphate (pH 7.0), 20 °C]. Spectra were recorded before heating (black curves) and after heating to 90 °C and cooling back to room temperature (red curves).

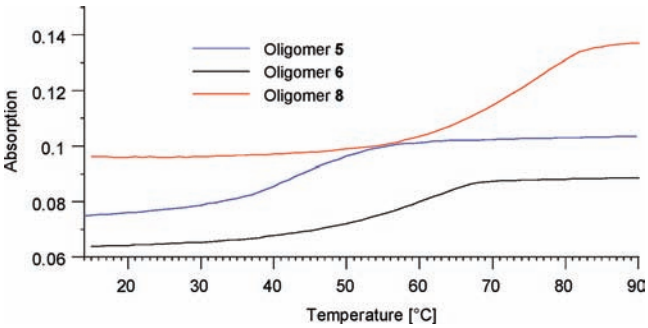

Figure 5. Thermal denaturation of oligomers **5**, **6**, and **8** at 1 μM concentration [conditions: 10 mM phosphate (pH 7.0), 3.0 M NaCl; absorbance monitored at 282 nm]. For clarity, only the third ramp of a cooling−heating−cooling cycle is shown for each oligomer.

The changes in the CD spectra of the oligomers are remarkable. Two markedly different structural conformations exist at medium (0.5−1.5 M NaCl) and high (2−4 M NaCl) salt concentrations for oligomers **5** and **8**. The same behavior was observed for the enantiomeric oligomers **4** and **7** (see the SI). Generally, all of the oligomers with (*S*,*S*)-linkers gave rise to an intensive negative band at 240 nm at high salt concentration (e.g., oligomers **5** and **8**; Figure 2). This band changed to a positive signal at medium salt concentrations for oligomers **5** and **8**, but oligopyrene **6** did not exhibit this polymorphic behavior.

Denaturation Experiments. The hybridization process of the oligomers was monitored at different wavelengths (245, 282, and 365 nm). Cooperative melting was observed for all hybrids with exception of **3**, for which no transition was observed. Figure 5 shows the denaturation curves at 282 nm for oligomers **5**, **6**, and **8**. The folding process was entirely reversible. No differences could be observed by CD during several heating/cooling cycles. As can be seen in Figure 6, the spectra recovered completely after denaturation at 90 °C and re-equilibration at ambient temperature. For all of the oligomers, the denaturation curves and corresponding melting temperatures (T_m) were dependent on oligomer concentration (see the SI), which rules out monomolecular structures. Thus, the oligomers form multimeric hybrids under the conditions tested.

The formation of double-stranded helices in chimeric DNA−pyrene oligomers has been shown.[38,60,65] Such types of double-helical structures are most likely also to be formed by the present oligopyrenotides. The obtained T_m values show good correlations in van't Hoff plots [$1/T_m$ vs ln(C)],[66] as displayed in Figure 7. Values of the thermodynamic parameters derived

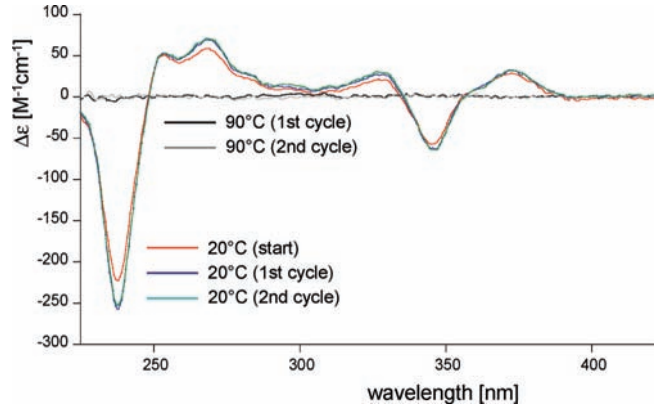

Figure 6. CD spectra of oligomer **5** taken before and after repeated heating to 90 °C. Spectra were taken after equilibration for 30 min at each temperature.

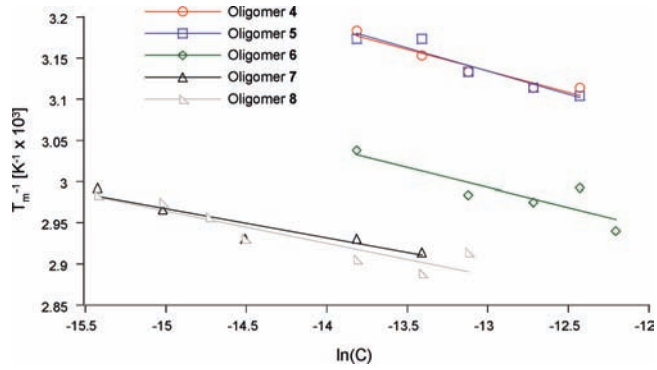

Figure 7. van't Hoff plots of $1/T_m$ vs ln(C) for oligomers **4**−**8**.

from these plots are given in Table 1.[67] Hybridization is enthalpy-driven. The van't Hoff enthalpy values (ΔH_{vH}) range between approximately −2 and −3 kcal/mol, while the entropies ΔS_{vH} are between −4.5 and −7.5 cal mol^{-1} K^{-1} per interstrand stacking interaction (also see the SI). These values are smaller than the average stacking enthalpies and entropies per base pair observed for double-stranded oligonucleotides of comparable length, which are on the order of −8 kcal/mol and −20 cal mol^{-1} K^{-1}, respectively.[68] The difference can be attributed, at least in part, to a reduction in the aromatic surface area involved in stacking interactions and by the absence of hydrogen bonds. Formation of other helical hybrids is a further possibility. In particular, triple helices based on pyrene interstrand stacking are imaginable (see the SI). Model considerations show that four-stranded hybrids are unlikely to form via interstrand stacking, at least with the type and length of interpyrenotide linkers used in the present oligomers.

Control of Helicity. Pyrene components are achiral. The 1,2-diaminocyclohexane unit serves as the chiral point of reference according to which the pyrene double strand adopts its

(66) Marky, L. A.; Breslauer, K. J. *Biopolymers* **1987**, *26*, 1601–1620.
(67) van't Hoff analysis is generally based on the assumption that ΔH is temperature-independent (e.g., see ref 66). As in the case of nucleic acid hybridization, this assumption may not be entirely correct. For example, see: (a) Rouzina, I.; Bloomfield, V. A. *Biophys. J.* **1999**, *77*, 3242–3251. (b) Mikulecky, P. J.; Feig, A. L. *Biopolymers* **2006**, *82*, 38–58. Nevertheless, van't Hoff analysis renders a first approximation of the thermodynamic data for the formation of a double-stranded oligopyrenotide hybrid.
(68) SantaLucia, J. *Proc. Natl. Acad. Sci. U.S.A.* **1998**, *95*, 1460–1465.

Table 1. Thermodynamic Parameters for Bimolecular Hybrid Formation of Oligopyrenotides

oligomer	sequence[a]	T_m [°C][b]	ΔH [kcal mol^{-1}][d]	$T\Delta S$ [kcal mol^{-1}][d,e]	ΔG [kcal mol^{-1}][d,e]
3	(*S*,*S*)-(Py)$_4$	–[c]	–	–	–
4	(Py)$_4$-(*R*,*R*)-(Py)$_4$	41	−38.4	−27.7	−10.7
5	(Py)$_4$-(*S*,*S*)-(Py)$_4$	42	−35.3	−24.8	−10.4
6	(*S*,*S*)-(Py)$_7$	56	−41.1	−28.5	−12.6
7	(Py)$_7$-(*R*,*R*)-(Py)$_7$	68	−55.6	−39.6	−16.0
8	(Py)$_7$-(*S*,*S*)-(Py)$_7$	71	−51.1	−35.6	−15.4

[a] (*S*,*S*) and (*R*,*R*) stand for the respective isomers of 1,2-diaminocyclohexane and Py for the pyrene building block (see Figure 1). [b] Melting temperatures at an oligomer concentration of 1 μM (exptl error ±1 °C). Conditions: 10 mM phosphate (pH 7.0), 3.0 M NaCl; absorbance was measured at 282 nm. [c] No T_m was observed. [d] Enthalpies, entropies, and free energies obtained from van't Hoff plots [$1/T_m$ vs ln(C)] for self-complementary oligomers forming a bimolecular hybrid (also see the SI).[66] [e] Using T = 293 K.

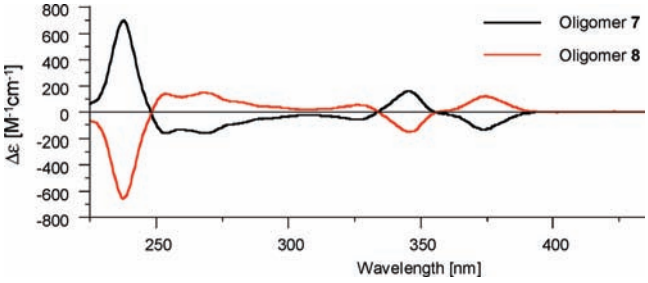

Figure 8. CD spectra of the enantiomeric pair of oligomers **7** and **8** at 3.0 M NaCl [5.0 μM oligomer concentration; 10 mM phosphate (pH 7.0)].

helicity.[7,69] The formation of enantiomorphic structures by pairs of two mutually enantiomeric oligopyrenes is shown in Figure 8. The CD spectra of **7** and **8** (as well as those of **4** and **5**; see the SI) are mirror-symmetric. Thus, control of extended left- or right-handed helices is effectively achieved by a single chiral building block. On the other hand, helicity can also be influenced by external factors, as evidenced by the remarkable change in the CD spectra at various salt concentrations (Figure 2). The origin of the apparent change in handedness induced by increasing the NaCl concentration from 1.5 to 3.0 M is difficult to assign. The salt concentration may have a direct effect on the stacking interactions of the pyrenes, or it may change the local structure of the glycol amide linkers. Furthermore, the pyrene carboxamide groups are also potentially involved in hydrogen bonding, and their conformations may be salt-dependent. In any case, a direct involvement of the chiral 1,2-diaminocyclohexane unit in the helical structure is likely, as inversion of helicity was observed in the oligopyrenotides in which this building block is located at an internal position (**5** and **8**) but not in **6**, in which it occupies a terminal, conformationally much less constrained position.[70]

Structural Parallels between Oligopyrenes and DNA. DNA is highly polymorphic. Depending on external factors, DNA of a given primary sequence can exist in different forms. In solution, the most common types are A-, B-, and Z-DNA. Interconversion between the different forms can be effected by changing various parameters, such as the degree of hydration (A-to-B transition)[22] or the ionic strength (B-to-Z transition).[71] Other secondary and tertiary structures include the G-quadruplex[72,73] and H-DNA.[74] The oligomers presented here are composed of repeating units of phosphodiester-linked pyrenes. Because of the obvious resemblance of this pattern to natural oligonucleotides, we refer to the units as *pyrenotides* (or, more generally, *arenotides*) and their oligomers as *oligopyrenotides* (*oligoarenotides*). The resemblance between oligopyrenotides and natural DNA goes beyond the formal similarity of the repetitive units, however. Just as in the DNA duplex, hybrids of oligopyrenotides are stabilized by hydrophobic and stacking interactions among the pyrenes, while the hydrophilic phosphate groups ensure water solubility. Figure 9 shows a minimized model as an illustration of a right-handed, homodimeric duplex structure of oligopyrenotide **5**. Hybrid formation and structural stability of oligopyrenotides is salt-dependent, as is the case for nucleic acids. Maybe most importantly, oligopyrenotides exhibit remarkable polymorphism, which is strongly reminiscent of DNA. A drastic change in helicity, comparable to the B-to-Z transition, is effected by altering the salt concentration. Because of these structural similarities to nucleic acids, oligoarenotides represent

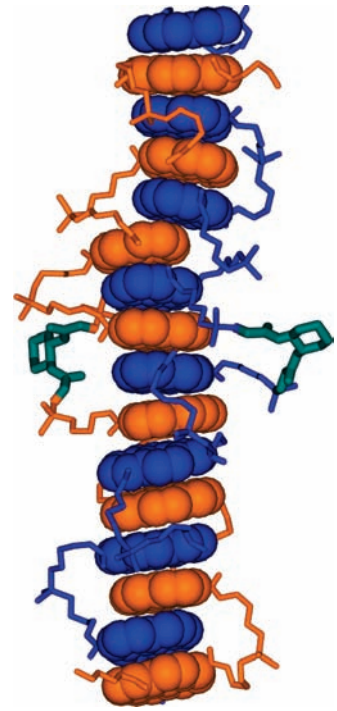

Figure 9. AMBER-minimized molecular model[80] of a right-handed homodimeric duplex formed by oligopyrenotide **5**. Alternating interstrand-stacked pyrenes are shown in blue and orange space-filling representations, and linkers between pyrenes are shown as sticks. (*S*,*S*)-1,2-Diaminocyclohexane units are shown in dark-green.

(69) Green, M. M.; Cheon, K. S.; Yang, S. Y.; Park, J. W.; Swansburg, S.; Liu, W. H. *Acc. Chem. Res.* **2001**, *34*, 672–680.
(70) For a discussion of environment-induced inversion of supramolecular chirality, see ref 62.
(71) Rich, A.; Nordheim, A.; Wang, A. H. J. *Annu. Rev. Biochem.* **1984**, *53*, 791–846.
(72) Sen, D.; Gilbert, W. *Nature* **1990**, *344*, 410–414.
(73) Williamson, J. R. *Annu. Rev. Biophys. Biomol. Struct.* **1994**, *23*, 703–730.
(74) Mirkin, S. M.; Frank-Kamenetskii, M. D. *Annu. Rev. Biophys. Biomol. Struct.* **1994**, *23*, 541–576.

a simplistic model of a self-replicating system. It is conceivable that primitive self-replicating systems could be based on hybridization through aromatic stacking interactions without mutual recognition of complementary bases via hydrogen bonding. Sequence information may be provided in mixed sequences, since the electronic and structural diversity present in different aromatic building blocks should favor certain types of stacking interactions.[75,76] Mixed sequences might therefore lead to sequence-specific hybridization even in the absence of specific hydrogen-bonding patterns.[77] In addition, oligopyrenotides possess a phosphodiester backbone similar to that of DNA and RNA. While the phosphodiester groups ensure water solubility of the oligomers, they may also be crucial for the formation of multistranded helices in polar environments. The importance of the polyanionic backbone for the proper functioning of DNA as a genetic molecule was pointed out by Benner and Hutter.[56] The polyelectrolyte backbone controls the degree of folding of the single strand and thereby ensures that the single strand can act as a template by formation of multistranded hybrids. Thus, although simple oligopyrenotides such as the ones presented here have little sequence information, they may serve as model compounds for the design of artificial, self-replicating systems.[27,78,79]

Conclusions

We have described abiotic, polyanionic oligomers called *oligopyrenotides* that exhibit remarkable structural analogies to DNA. They are composed of achiral, non-nucleosidic pyrene building blocks linked by phosphodiester groups. A single 1,2-diaminocyclohexane unit provides the chiral information leading to formation of homochiral helices.[7,62,69] The oligomers form stable hybrids in aqueous solution. Oligopyrenotides display salt-concentration-dependent structural polymorphism. Despite their chemical simplicity, oligopyrenotides possess a number of structural attributes typically observed in nucleic acids and therefore may serve as model compounds for the design of artificial self-replicating systems.

Experimental Section

General. Reagents used for synthesis of pyrene and chiral 1,2-diaminocyclohexane phosphoramidites were purchased from Fluka, Sigma-Aldrich, or Acros and used without further purification. Full experimental details and spectroscopic characterization data are provided in the SI.

Preparation of Oligomers. Oligomers were synthesized on a 394 DNA/RNA Synthesizer (Applied Biosystems) according to standard phosphoramidite chemistry ("trityl-off" mode). The pyrene and 1,2-diaminocyclohexane phosphoramidite building blocks were used as 0.1 M solutions in dichloromethane. The coupling time was elongated to 2 min. Cleavage from the pyrene-modified polystyrene solid support and final deprotection were achieved by treatment with 30% ammonium hydroxide at 55 °C overnight. The crude oligomers were purified by reversed-phase HPLC (LiChrospher 100 RP-18, 5 μm, Merck; Bio-Tek Instruments Autosampler 560) using eluent A = $(Et_3NH)OAc$ (TEAAc) buffer (0.1 M, pH 7.0) and eluent B = 80% acetonitrile/20% TEAAc buffer; elution was performed at 50 °C. Mass spectrometry (MS) data for the purified oligomers were obtained by electrospray ionization (ESI) MS in negative-ion mode (Applied Biosystems Sciex QTrap). For oligomer concentration determination, a value of $\varepsilon_{260\ nm} = 9000\ M^{-1}\ cm^{-1}$ per pyrene unit was used.

Thermal Denaturation Experiments. A Varian Cary 100 Bio-UV/vis spectrophotometer equipped with a Varian Cary block temperature controller and Varian WinUV software was used to determine the melting curves at 245, 282, and 365 nm (cooling−heating−cooling cycles over the temperature range 10−90 °C, temperature gradient 0.5 °C min^{-1}, optical path length 10 mm). Melting temperatures (T_m) were determined from the second cooling ramp of the cooling−heating−cooling cycle. The data were collected and analyzed with Kaleidagraph software from Synergy Software.

UV−Vis Spectra. UV−vis spectra were collected in quartz cuvettes with an optical path of 10 mm over the range 200−500 nm on a Varian Cary 100 Bio-UV/vis spectrophotometer equipped with a Varian Cary block temperature controller and Varian WinUV software.

Circular Dichroism Spectra. CD spectra were recorded on a JASCO J-715 spectropolarimeter equipped with a JASCO PFO-350S temperature controller. The samples were scanned at 50 nm min^{-1} with a bandwidth of 1 nm and a response time of 1 s over the 200−500 nm range at constant temperature. Each spectrum was taken as an average of three scans using a 10 mm cell. Values of $\Delta\varepsilon$ were determined by dividing the ratio of the measured ellipticity Θ (mdeg) and 32980 by the total oligomer concentration [i.e., $\Delta\varepsilon = \{\Theta\ [mdeg]/32980\}/(total\ oligomer\ concentration)$].

Fluorescence Experiments. Variable-temperature fluorescence data were collected on a Varian Cary Eclipse fluorescence spectrophotometer equipped with a Varian Cary block temperature controller (excitation at 354 nm; excitation and emission slit width of 5 or 2.5 nm, detector sensitivity of 600 or 800 V). Varian Eclipse software was used to investigate the fluorescence of the different oligomers over the wavelength range 365−680 nm. The data were collected and analyzed with Kaleidagraph software from Synergy Software.

Molecular Modeling. The model of a duplex composed of oligomer **5** (Figure 9) was generated using HyperChem 7.5.[80] Geometry optimization (in vacuum) was carried out using the AMBER force field. After solvation of the structure (geometry optimization in solution with the AMBER force field) and use of molecular dynamics to anneal the system, reoptimization of the geometry using the AMBER force field was performed.

Acknowledgment. This work was supported by the Swiss National Foundation (Grant 200020-117617).

Supporting Information Available: Synthetic procedures; analytical details; melting curves; and UV−vis, fluorescence, and CD spectra. This material is available free of charge via the Internet at http://pubs.acs.org.

JA102042P

(75) Hunter, C. A.; Sanders, J. K. M. *J. Am. Chem. Soc.* **1990**, *112*, 5525–5534.
(76) Meyer, E. A.; Castellano, R. K.; Diederich, F. *Angew. Chem., Int. Ed.* **2003**, *42*, 1210–1250.
(77) Langenegger, S. M.; Häner, R. *Bioorg. Med. Chem. Lett.* **2006**, *16*, 5062–5065.
(78) Wu, Y. Q.; Ogawa, A. K.; Berger, M.; McMinn, D. L.; Schultz, P. G.; Romesberg, F. E. *J. Am. Chem. Soc.* **2000**, *122*, 7621–7632.
(79) Krueger, A. T.; Lu, H. G.; Lee, A. H. F.; Kool, E. T. *Acc. Chem. Res.* **2007**, *40*, 141–150.
(80) *HyperChem*, release 7.5; Hypercube, Inc.: Gainesville, FL, 2003.